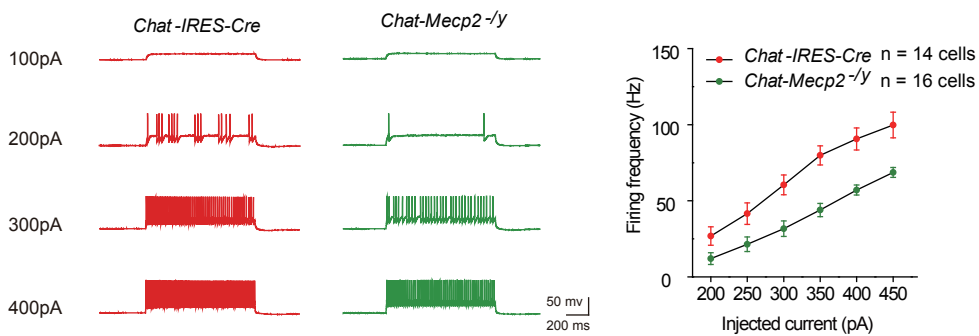
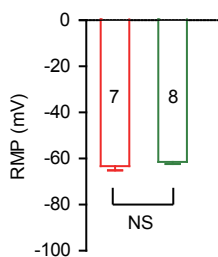


Supplementary Figure - 4 Li

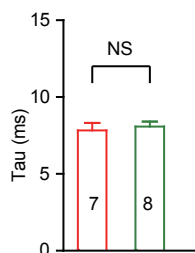
A



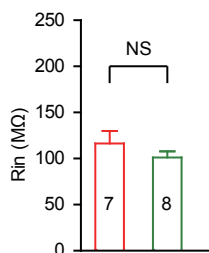
B



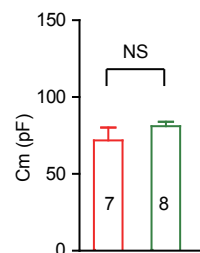
C



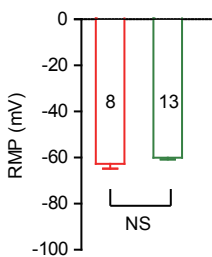
D



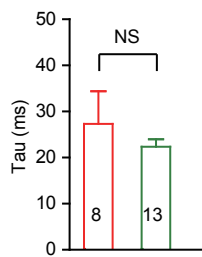
E



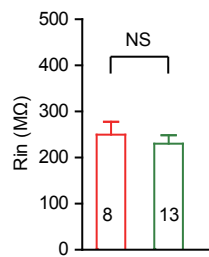
F



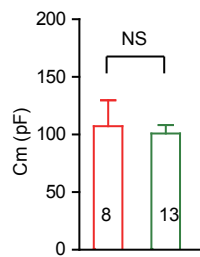
G



H



I



Supplementary Figure 4. *Chat-Mecp2^{-/-}* mice exhibited increased activity of PV interneurons in the hippocampus but no statistical difference in passive membrane properties either in PV interneurons or pyramidal neurons. **A**, Left, Voltage responses to various current injection steps (1 s) in hippocampal PV interneurons from *Chat-IRES-Cre* and *Chat-Mecp2^{-/-}* mice. Right, Plot of firing frequency in a train elicited in response to a 1 s suprathreshold current of 200 to 450 pA in *Chat-IRES-Cre* and *Chat-Mecp2^{-/-}* mice. **(B-E)** Quantitative analysis of resting membrane potential (RMP), membrane time constant (τ), input resistance (Rin) and membrane capacitance (Cm) of PV interneurons in slices from *Chat-IRES-Cre* and *Chat-Mecp2^{-/-}* mice. **(F-I)** Quantitative analysis of resting membrane potential (RMP), membrane time constant (τ), input resistance (Rin) and membrane capacitance (Cm) of pyramidal neurons in hippocampal slices from *Chat-IRES-Cre* and *Chat-Mecp2^{-/-}* mice. *P*-values were calculated by two-sided t-test. Error bars are means \pm s.e.m.